tvst

Article

A Smart Vitrector Equipped by a Fiber-Based OCT Sensor Mitigates Intentional Attempts at Creating Iatrogenic Retinal Breaks During Vitrectomy in Pigs

Alexandre Abid[1,2], Renaud Duval[3,4], Flavio Rezende[3,4], and Christos Boutopoulos[1,2,4]

[1] Institute of Biomedical Engineering, University of Montreal, Montreal, Quebec, Canada
[2] Maisonneuve-Rosemont Hospital Research Centre, Montreal, Quebec, Canada
[3] Maisonneuve-Rosemont Hospital, Montreal, Quebec, Canada
[4] Department of Ophthalmology, University of Montreal, Montreal, Quebec, Canada

Correspondence: Christos Boutopoulos, 5690 Rosemont Blvd, Montreal, Quebec, H1T 2H2, Canada. e-mail: christos.boutopoulos@umontreal.ca

Received: January 19, 2021
Accepted: October 8, 2021
Published: November 12, 2021

Keywords: vitrectomy; smart vitrector; optical fiber probe; iatrogenic retinal injury; optical coherence tomography; vitreoretinal surgery

Citation: Abid A, Duval R, Rezende F, Boutopoulos C. A smart vitrector equipped by a fiber-based OCT sensor mitigates intentional attempts at creating iatrogenic retinal breaks during vitrectomy in pigs. Transl Vis Sci Technol. 2021;10(13):19, https://doi.org/10.1167/tvst.10.13.19

Purpose: The occurrence of iatrogenic retinal breaks (RB) in pars plana vitrectomy (PPV) is a complication that compromises the overall efficacy of the surgery. A subset of iatrogenic RB occurs when the retina (rather than the vitreous gel) is cut accidentally by the vitrector. We developed a smart vitrector that can detect in real-time potential iatrogenic RB and activate promptly a PPV machine response to prevent them.

Methods: We fabricated the smart vitrectors by attaching a miniaturized fiber-based OCT sensor on commercial vitrectors (25G). The system's response time to an iatrogenic RB onset was measured and compared to the literature reported physiologically limited response time of the average surgeon. Two surgeons validated its ability to prevent simulated iatrogenic RB by performing PPV in pigs. Note that the system is meant to control the PPV machine and requires no visual or audio signal interpretation by the surgeons.

Results: We found that the response time of the system (28.9 $\pm$ 6.5 ms) is 11 times shorter compared to the literature reported physiologically limited reaction time of the average surgeon ($P < 0.0001$). Ex vivo validation (porcine eyes) showed that the system prevents 78.95% (15/19) (95% confidence interval [CI] 54.43–93.95) of intentional attempts at creating RB, whereas in vivo validation showed that the system, prevents 55.68% (30/54) (95% CI 41.40–69.08), and prevents or mitigates 70.37% (38/54) (95% CI 56.39–82.02) of such attempts. A subset of failures was classified as "early stop" (i.e., false positive), having a prevalence of 5.26% (1 /19) in ex vivo tests and 24.07% (13/54) in in vivo tests.

Conclusions: Our results indicate the smart vitrector can prevent iatrogenic RB by providing seamless intraoperative feedback to the PPV machine. Importantly, the use of the smart vitrector requires no modifications of the established PPV procedure. It can mitigate a significant proportion of iatrogenic RB and thus improve the overall efficacy of the surgery.

Translational Relevance: Potential clinical adoption of the smart vitrector can reduce the incidence of iatrogenic RB in PPV and thus increase the therapeutic outcome of the surgery.

Introduction

Pars plana vitrectomy (PPV) is a frequent ocular surgery involving removal of the vitreous gel from the eye and repair of the retina.[1] By allowing controlled access to the posterior segment of the eye, pars plana vitrectomy has dramatically changed the management of diseases of the retina. In PPV, surgeons manipulate surgical instruments inside the vitreous cavity, in close proximity to the retinal layer, thereby risking its injury.[2,3] A recent meta-analysis of surgical

complications of primary rhegmatogenous retinal detachment has reported rates of iatrogenic retinal breaks (RB) ranging from 7.7% to 10% of surgeries.[3] Those RB are particularly important because they may lead to failure of the surgery if not recognized and appropriately dealt with.

The vitrector or "cutter" is the central intraocular tool in PPV, integrating the functions of vitreous gel cutting and aspiration. Surgeons control the positioning of the vitrector inside the eye with their dominant hand and use a foot pedal to activate/deactivate its cutting and aspiration function. A crucial step during PPV for retinal detachment is the "shaving" of the vitreous base. During this maneuver, the vitrector is brought in very close proximity to the retina while simultaneously aspirating and cutting the vitreous. The closer the vitreous base is shaved to the retina, the more effective the surgery is, with the caveat of a higher risk of iatrogenic injury to the retina.

A subset of iatrogenic RB occurs when retina is inadvertently aspirated and cut by the vitrector before the surgeon has time to stop the action of the vitrector by releasing the controlling foot pedal. Surgeons' reaction time to such events is limited for physiological and anatomical reasons within the range of 300 to 400 ms.[4,5] Given that the usual cutting speed for retina shaving ranges from 5000 to 16,000 cuts per minute,[6] the guillotine of the vitrector can move and "cut" at least 33 to 106 times before deactivation, resulting in retinal damage. The exact prevalence of this potentially avoidable cause of iatrogenic RB remains unknown.

Existing approaches to mitigate iatrogenic retinal breaks mainly rely on selecting operating settings that reduce vitreoretinal traction. These include reducing the vacuum, as well as increasing the cutting speed.[7] The selection of low duty cycle (i.e., cutter on/cutter off time) is also used to reduce vitreoretinal traction[8] and thus to mitigate iatrogenic RB. This approach, known as "shave mode," is enabled by dual pneumatic control of the guillotine movement. Although effective in reducing vitreoretinal traction, these approaches are ultimately limited by the reaction time of the surgeons. Presently, none of the available mitigation technologies focus on eliminating surgeons' rection time.

Optical coherence tomography (OCT) systems employ a technique known as low-coherence interferometry to generate tomographic images of tissue.[9] Fiber-based endoscopic OCT probes have been used as complementary visualization tools for eye surgery.[10,11] Moreover, fiber-based OCT probes attached to surgical instrumentation can provide real-time positioning feedback, as well as tremor compensation capabilities. Previous implementations of "smart" OCT-enabled ophthalmic systems include tremor cancellation microinjectors[12] and microforceps.[13]

Here we demonstrate a semiautomated type of PPV based on a smart vitrector, where the most timing-sensitive manipulation toward preventing iatrogenic RB (i.e., "cutter" and aspiration deactivation via pedal release) is assigned to a fast risk-detection algorithm. To implement the smart vitrector, we used an OCT-based miniaturized intraocular fiber sensor, attached to a commercial vitrector, to detect in real-time potential iatrogenic RB and activate promptly a PPV machine response to prevent them. The smart vitrector does not require the surgeon to interpret intraoperatively a visual, audio, or other type of software-generated signal. We present a complete description of the system, including the optical sensor fabrication process, the smart vitrector assembling and the decision-making algorithm. Furthermore, we report system response time measurements, as well as pig model validation results ex vivo and in vivo.

Methods

OCT Probe Design and Fabrication

We used commercially available fibers (SM: SM800-5.6-125, GRIN: GIF625; Thorlabs, Newton, NJ, USA) and telecom splicing/cleaving equipment (AI-6; Signal Fire, Chengdu, China) for the fabrication of the OCT probes.[14] The thickness of the probes was 125 µm. We sought for a probe that focuses the exiting beam at 260 µm from its distal tip once immersed in the vitreous. Given the size of the vitrectors' orifice, such an approach provides maximum detection sensitivity right above its central part. We used a theoretical model[14] to design such probes and opted for a 320 µm GRIN fiber component to attain the desired focusing. Each probe was spliced to a 2 m–long SM fiber FC/APC patch cable. A schematic representation and an optical microscopy image of a typical probe can be found in Figures 1a and 1b.

Smart Vitrector Assembly

Precise attachment and alignment of the OCT probe on the vitrector is crucial to efficiently detect the movement of the retina towards the cutter. After a series of pilot tests, we opted for the assembly shown in Figures 1c to 1f, where the probe distal tip points in front of the vitrector's orifice. Note that a 100 µm to 200 µm distance was kept between probe distal tip and the closest end of the vitrector's orifice. Such a

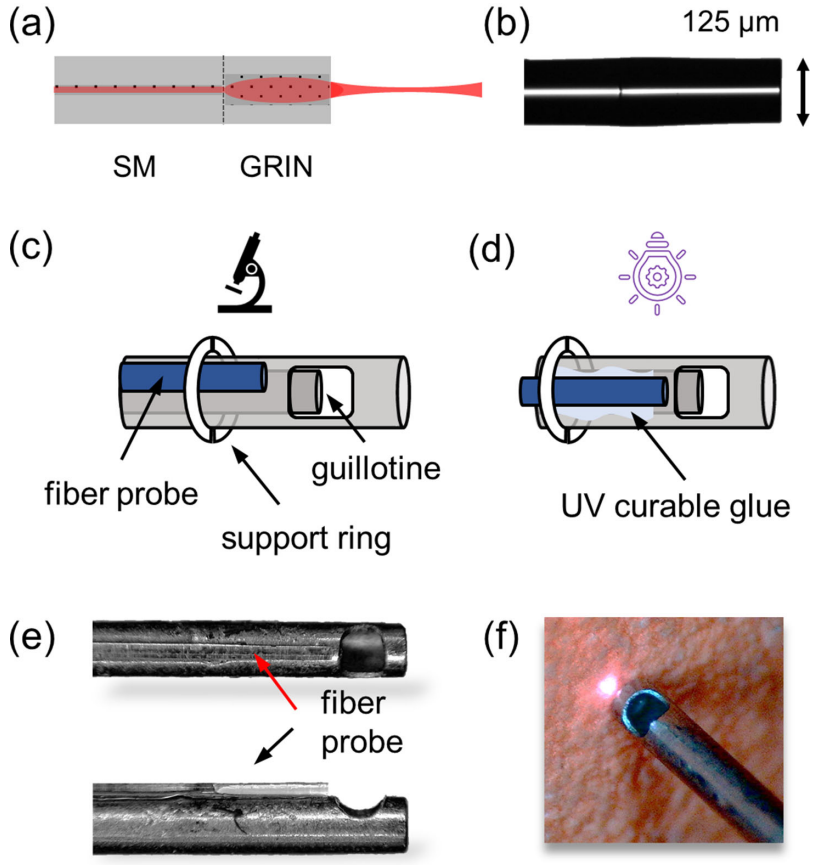

Figure 1. Schematics and photographs of the fiber probe/vitrector assembly. (a) Schematic drawing and (b) optical microscopy image of a 125 µm–thick probe composed of an SM and a GRIN fiber. Schematic drawings demonstrating the assembling steps of (c) alignment and (d) gluing. (e) Top and side view of the fiber probe/vitrector assembly and (f) the trace of the exiting beam on a near-infrared card.

design allows for direct sensing of a mobile retina heading towards the guillotine. The assembling protocol consisted in two steps (Figs. 1c, 1d). First, we mounted 25-gauge vitrectors (MID Labs, San Leandro, CA, USA) and fiber probes on separate translation stages and aligned them under a microscope (Fig. 1c). We used home-made plastic rings (i.e., pieces of pipette tips) to facilitate the alignment process. Second, once the desired alignment was achieved, we applied a medical device adhesive product (AA3922; Loctite, Henkel Corporation, Westlake OH, USA) along the fiber probe/vitrector interface and cured with a UV light (Fig. 1d). Care was taken not to cover the tip of the probe with glue. Figure 1e shows top-view and side-view optical microscopy images of a typical vitrector/fiber probe assembly, whereas the trace of the near-infrared exiting laser beam on a card detector is shown in Figure 1f. The thickness of the modified vitrectors ranged from 0.65 mm to 0.7 mm, depending on the thickness of the glue layer, which varied from 0.025 mm to 0.075 mm.

OCT System

For the ex vivo experiments we used a home-made spectral-domain OCT (SD-OCT) setup, operating at 840 nm central wavelength and providing A-scans at 100Hz. A detailed description of the system can be found in our previous work.[14] For the in vivo experiments we used an upgraded home-made SD-OCT system providing A-scans at 500Hz (Figs. 2a, 2b). The use of a compact laser source in combination with a faster spectrometer was the key upgrade of the in vivo system. The system uses a SLED light source (central wavelength: 880 nm; bandwidth: 70 nm, EXS210088-02; Exalos, Schlieren, Switzerland) powered by a compact diver board (EBD 5020; Exalos), a spectrometer (AvaSpec-ULS4096CL-EVO; Avantes, Apeldoorn, the Netherlands), a 50:50 fiber coupler (AC Photonics Inc, Santa Clara, CA, USA) and a variable optical attenuator (V800A; Thorlabs) (Fig. 2a). We used a LabVIEW-based program to control the system. We applied the following signal processing steps to acquire

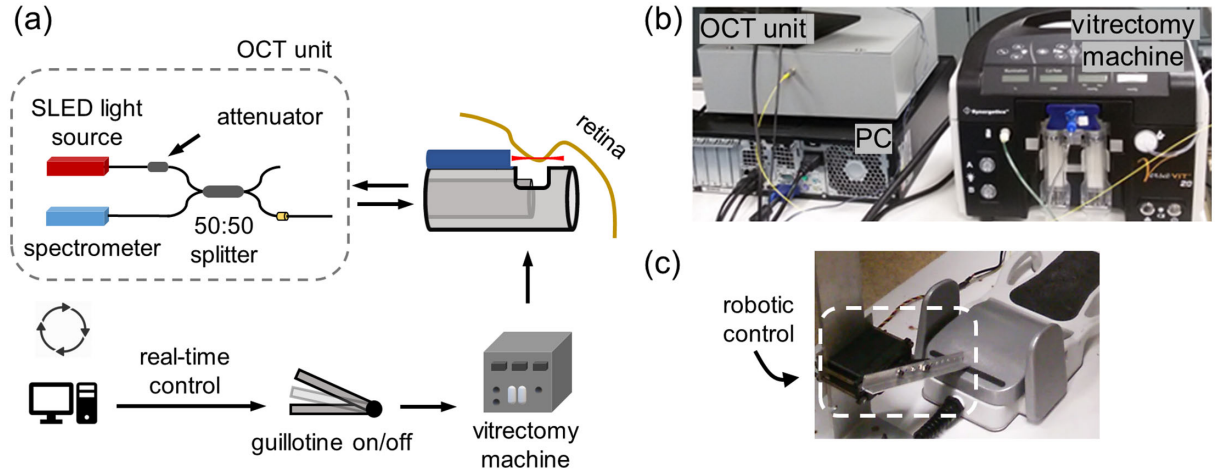

Figure 2. The smart vitrectomy system. (a) Schematic representation of the OCT unit and overview of the injury prevention mechanism. Images of the experimental setup, including (b) the OCT unit, the personal computer (PC), the vitrectomy machine, and (c) the robotic mechanism (i.e., servomotor and metallic beam) used to control the pedal.

A-scans: (a) evenly spaced wavelength data were converted into evenly k-spaced data with linear interpolation; (b) the raw interferogram was filtered with a high-pass filter to remove the DC component and then with a low-pass filter to remove the high-frequency noise; (c) fast Fourier transform was then applied to the filtered interferogram to acquire A-scans of the sample. We interrogated the presence of the retina in front of the vitrector's orifice by real-time processing of A-scans. Both ex vivo and in vivo OCT systems were used in a common path configuration, where the reference signal originates from the partial reflection of the light at the probe-vitreous interface. The selection of a common path configuration provides key advantages for our setting. First, the absence of a reference arm keeps the OCT setup simple and compact. Second, probe/vitrector assemblies of arbitrary length can be easily interchanged without necessitating changes of the OCT system (i.e., refence arm adjustment).

Retinal Detection Algorithm and Injury Prevention System

During a conventional vitrectomy, surgeons control the cutting function of the vitrector by a foot pedal connected to a vitrectomy machine. In our work, we assigned this task to a simple robotic arm (Fig. 2c), controlled by a retinal detection algorithm via a microcontroller (Arduino Pro Mini 328; SparkFun Electronics, Niwot, CO, USA). The robotic arm consisted of a 10 cm metallic beam attached to a servomotor (HS-755HB; Hitec RCD, San Diego, CA, USA). The launch of the pedal initiates the cutting function of the vitrector (i.e., guillotine movement). During PPV surgery and on detection of a dangerous situation (e.g., the retina is sucked into the cutter), the foot pedal must be quickly released to prevent a retinal injury. We programmed the robotic arm to release the pedal once the OCT system would detect the presence of retina in front of the vitrectors' orifice. The detection algorithm was based on the following steps: (a) An interrogating window was selected, z_{min} to z_{max}, corresponding to the length of the orifice (400 µm) (Fig. 3a). The z_{min} varied from 100 µm to 200 µm according to the positioning offset of each attached probe in respect to the orifice. The z_{max} was set to z_{min} + 400 µm. (b) The vitrector was positioned far from the retina (distance $z > 5$ mm) to acquire and store a reference A-scan, $I_{ref}(z)$ (Fig. 3b). (c) We compared $I_{ref}(z)$, with intraoperative A-scans (Fig. 3c), I(z), in real time (i.e., 100 Hz or 500 Hz depending on the OCT unit). (d) When at least 2% of the wavenumbers within the interrogated window met the condition $I(z) > S \times I_{ref}(z)$, where S was a user defined parameter, deactivation of the pedal was triggered. Such a programming approach enabled us to interrogate the presence of retina covering at least any 2% of the vitrector's orifice length. Figure 3d shows typical A-scans collected during vitrectomy on a pig, where $I_{ref}(z)$ and I(z) can be appreciated. In this example, I(z) corresponds to a PPV maneuver in which a detached retina moved toward the orifice and triggered the deactivation of the pedal.

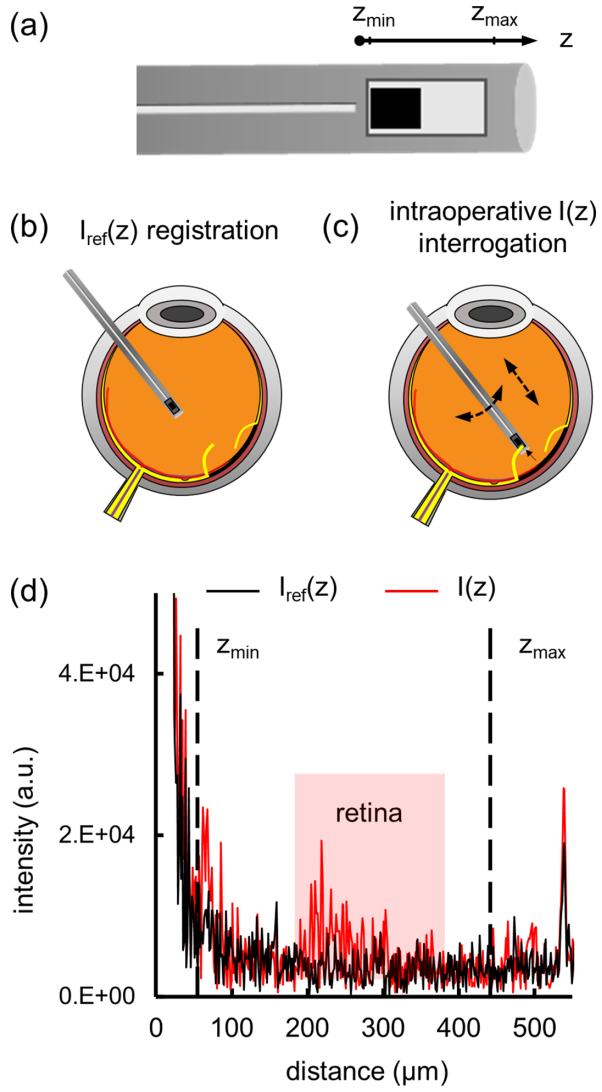

Figure 3. Overview of the intraoperative retinal detection. (a) Schematic drawing showing the vitrector fiber assembly and the interrogation window. Schematic drawings showing (b) the process of registering a reference A-scan and (c) the intraoperative interrogation of the retinal presence in front of the vitrector's orifice. (d) Indicative A-scans acquired during vitrectomy on a pig with (*red*) or without (*black*) the presence of the retina in front of the vitrector's orifice.

Measurement of System's Response Time

To acquire the system's response time, we used the setup shown in Figure 4a and the following steps: (a) a triggering A-scan was generated via passing the probe-exiting beam through a cover slip (to generate a triggering event similar to retina detection), (b) the onset of the triggering event was captured with the help of a mechanical shutter and a photodiode, c) the corresponding onsets of the digital-to-analog converter (Labjack U3; LabJack, Lakewood, CO, USA) response (i.e., intermediate) and the robotic arm/pedal response (i.e., overall) were recorded. A representative simultaneous recording of the intermediate and overall response time is shown in Figure 4b. We performed 20 recordings to calculate the average response time and its standard deviation.

PPV on Porcine Cadaver Eyes

Freshly enucleated porcine eyes were placed on an eye holder. In a preliminary series of experiments, we observed poor imaging of the retina because of partial cornea opacity. Therefore we opted for removing the anterior segment to improve imaging. Vitrectomy maneuvers were performed using a VersaVIT 2.0 machine (Synergetics USA, O'Fallon, MO, USA) and modified 25-gauge vitrectors (Synergetics procedure pack, 70025S; Synergetics USA). The surgeon operated using the modified vitrector with or without activating the smart vitrector system. One surgeon (surgeon 1) performed 19 aggressive approaches with an intention to injure ("bite") the retina with the system "On." The surgeon operated close to both attached retina and detached/torn retina and evaluated the outcome of each approach. Three approaches were performed with the system "Off." We used three evaluation scores: (i) retinal injury prevention (i.e., on-time deactivation of the cutter just before cutting the retina), (ii) retinal injury (i.e., no cutter de-activation at all, "retinal bite"), and (iii) early stop (i.e., deactivation of the "cutter" far from the retina–false positive). We filmed all approaches and used the videos to confirm the evaluation of the surgeon.

Pig Eye Surgeries

The in vivo study was performed in accordance with the ARVO Statement for the Use of Animals in Ophthalmic and Vision Research, following an approval by the animal ethics committee of the Maisonneuve-Rosemont Hospital Research Centre (Project 2019-1481). Two surgeons performed experimental PPV on two pigs (one bilateral and one unilateral) using the equipment described above. Pigs underwent surgeries under general anesthesia. A standard three-port PPV setting was used. We used a 20-gauge trocar for the insertion of the modified vitrector. To set challenging conditions, retinal detachments were induced by subretinal injection of a saline solution and retinal tears by using the tip of the light pipe. Iatrogenic RB were simulated by aggressive "shaving" approaches of the smart vitrector towards the retina with an intention to injure ("bite") it. The surgeons performed a total of 54 test PPV approaches with the

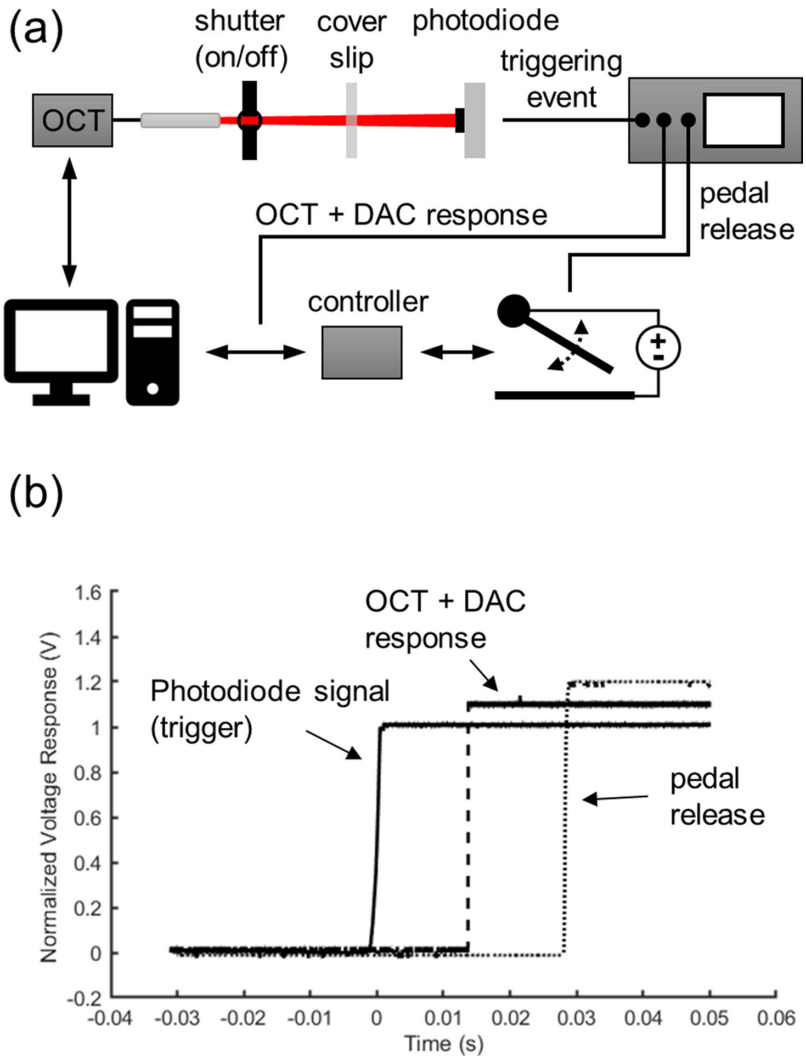

Figure 4. Overview of the response time measurement approach. (a) Schematic drawing of the setup used to measure the response time of the OCT system and robotic arm. (b) Representative recordings of the intermediate (i.e., due to software and USB latency) and overall response time (i.e., detection to pedal release). The signal corresponding to pedal release signal has been inverted.

system "On" (surgeon 1: 17; surgeon 2: 28) and a total of three approaches with the system "Off" (surgeon 1: 1; surgeon 2: 2). They used the following range of vitrectomy machine settings (Supplementary Table S1): vacuum: 50 to 200 mm Hg, cutting rate: 5000 cuts per minute and 6000 cuts per minute (max limit of the machine). Thirty-six of 54 approaches were initiated toward detached and torn retina, a condition representing one of the most challenging PPV tasks. Similar to the ex vivo work, they used the primary evaluation scores of (i) retinal injury prevention, (ii) retinal injury, and (iii) early stop. Given that the visualization was greatly improved compared to ex vivo testing, surgeons were able to classify some approaches as (iv) late stop. "Late stop" represented any of the following outcomes: (a) the cutter stopped, but the retina was sucked into the orifice and exited without obvious injury, or (b) the cutter stopped, but the retina was sucked in and a minor cut was identified.

Statistics

Unpaired Student's *t*-test was used to compare the response time of the OCT system compared to that reported for surgeons. For the validation tests, we calculated 95% binomial proportion confidence interval using the Clopper-Pearson exact method.

Results

The Overall Response Time of the System is 11 Times Faster Compared to That Reported for Surgeons.

By using the system described in Figure 4, we found that the intermediate response time of the in vivo system (i.e., attributed to the spectrometer, software and USB latency) was 14.2 ± 4.4 ms (N = 20) and that the overall response time (i.e., from detection to pedal release) was 28.9 ± 6.5 ms (N = 20). Note that the use of test sample (i.e., cover slip) was essential to determine the response time of the system. However, the response time is independent of the material sensed. The overall response time is 11 times faster compared to the physiologically limited reaction time of the "average" surgeon[4,5] ($P < 0.0001$). The literature value considered for this comparison is 328.7 ± 48.7 ms and represents the average response of 47 subjects to a visual cue ("light on").[5] The experimental protocol required the use of a surgical microscope by the participants to mimic a surgical environment.[5] These results indicate that our approach can significantly reduce the number of non-desirable "cuts" of the vitrector after the detection of a dangerous situation (e.g., retina traction). For example, for a cutting rate of 5000 cuts per minute, post-detection movement of the guillotine can be reduced from 33 "cuts", which corresponds to the average surgeon reaction time, to ~ 2.4 "cuts". By considering the average speed of tool movement during vitreoretinal surgery simulations,[15] one can estimate that the vitrector would move ~ 45 µm on average before complete deactivation of the guillotine.

The Smart Vitrector Prevented 78.95% of Simulated Iatrogenic RB on Cadaver Porcine Eyes

In the first part of our work, we used enucleated porcine eyes to test the system. Of the 19 trials to exert damage to the retina, three (15.79%) resulted in damage, damage was prevented in 15 (78.94%), while one trial was classified as "early stop" (5.26%); corresponding to a success rate of 83.33% (95% confidence interval [CI] 58.58–96.42) when not considering the "early stops" or 78.95% (95% CI 54.43–93.95) using an "early stop equals failure" approach (Fig. 5). Naturally, three out of three trials induced damage when the smart vitrector was deactivated (Fig. 5). Indicative videos of vitrector-retina approaches with and without activating the smart vitrector system are provided in the Supplementary Material (Supplementary Videos S1 and S2).

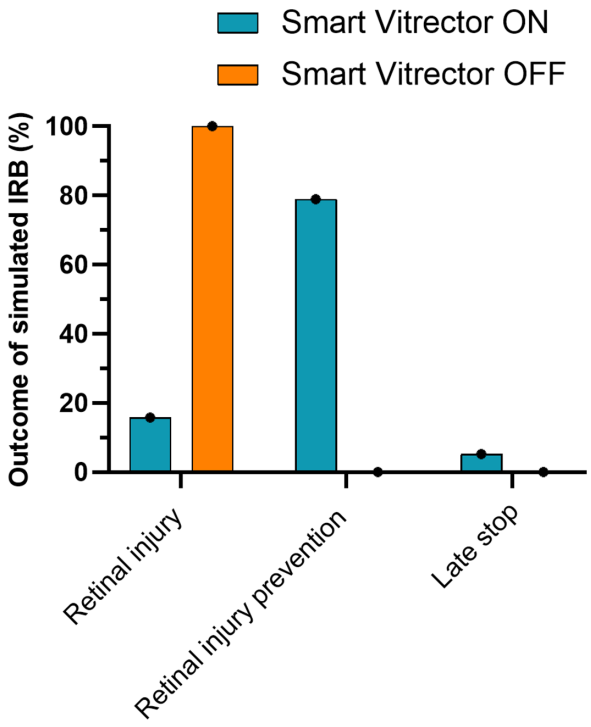

Figure 5. Outcome of simulated iatrogenic retina breaks on cadaver porcine eyes. Nineteen approaches were performed with the smart vitrector system "On" and three with the smart vitrector system "Off."

The Smart Vitrector Prevented 55.56% of Simulated Iatrogenic RB in Pig Surgeries.

In the second part of our work, we sought to validate our system in the context of an animal surgery operating room, where instrumentation, time constrains and physiological responses (i.e., bleeding) simulate those encountered in a clinical setting. A detailed description of the PPV experimental settings and outcome can be found in Supplementary Material Table S1. Figures 6a to 6c show a sequence of images representative of an injury prevention, whereas Figures 6d to 6f show a sequence of images representative of an "early stop" triggered by blood flow. The corresponding videos can be found as Supplementary Material (Supplementary Videos S3 and S4).

Figure 7 summarizes the outcome of the surgeries. Of the 54 trials to exert damage to the retina, 11 (20.37%) resulted in damage, damage was prevented in 30 (55.56%), while 13 (24.07%) trials were classified as "early stops"; corresponding to a success rate of 73.17% (30/41) (95% CI 57.06–85.78) when not considering the "early stops" or 55.68% (30/54) (95%

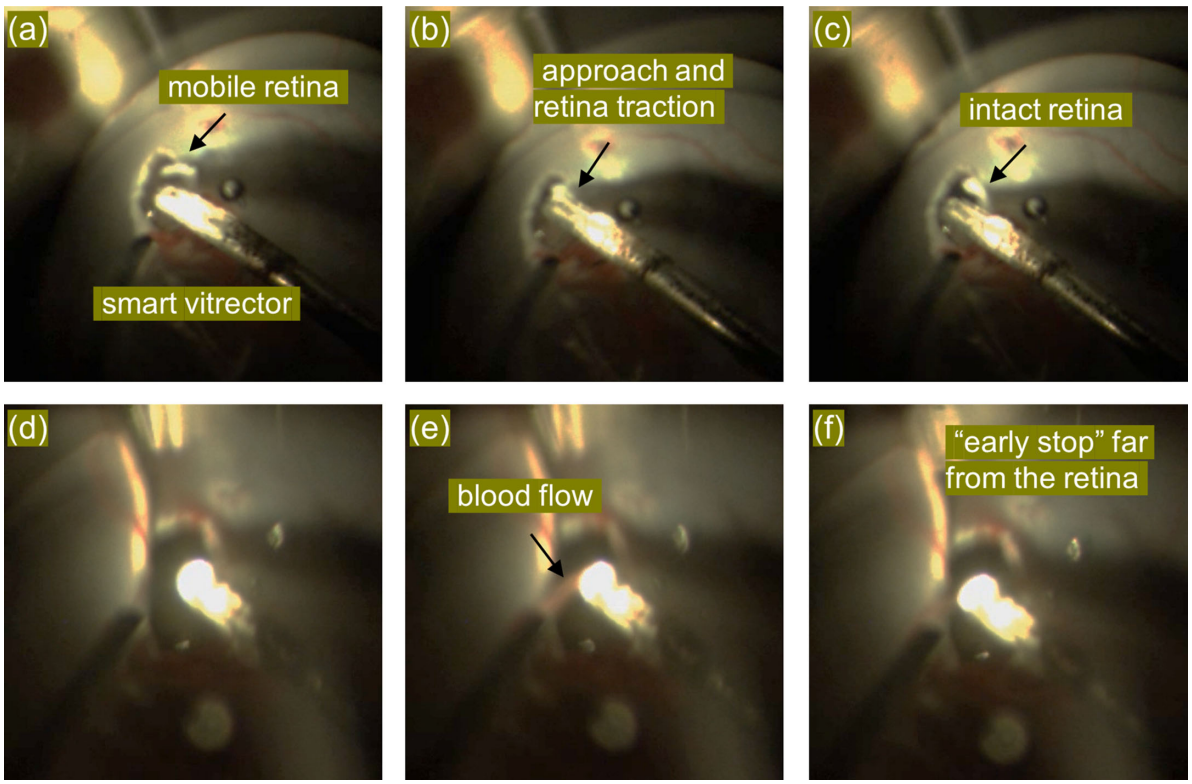

Figure 6. Visualization of trials simulating iatrogenic retinal breaks. (a–c) Indicative frames from Supplementary Video S3 showing a successful prevention of retinal injury. (d–f) Indicative frames from Supplementary Video S4 showing an "early stop," that is, deactivation of the cutter due to blood flow. In Supplementary Videos S3 and S4, a characteristic sound can be appreciated for frames (b) and (e), corresponding to the automated pedal release.

CI 41.40–69.08) using an "early stop equals failure" approach. Considering the secondary classification of "late stops", the system prevented or mitigated 92.68% (95% CI: 80.08–98.46) of attempts at creating retinal damage when not considering the "early stops" or 70.37% (38/54) (95% CI 56.39–82.02) using an "early stop equals failure" approach. Naturally, three out of three trials induced damage when the smart vitrector was deactivated. Altogether, these results indicate that clinical adoption of the smart vitrector can potentially eliminate or mitigate the subset of iatrogenic RB occurring when the retina (rather than the vitreous gel) is inadvertently aspirated and cut by the vitrector.

Discussion

We developed and validated a smart vitrector that mitigated intentional attempts at creating RB in pigs by providing seamless intraoperative feedback to the PPV machine. In surgeries performed with the smart vitrector, a timing-sensitive manipulation (i.e., the deactivation of the cutter) is assigned to a fast algorithm. In contrast to a variety of intraocular tools designed for other types of eye surgery[16–18] or operating microscopes integrating OCT capabilities,[11] surgeons do not have to interpret a visual or audio feedback for decision making. Importantly, the use of the smart vitrector requires no modifications (i.e., does not require additional ports or intraocular tools) of the established PPV procedure. As such, surgeons using the smart vitrector do not have to go through a learning curve or to change their usual operating style. Note that we used 20-gauge trocars for this work to accommodate the overall thickness of the 25-gauge based assembly (0.65–0.7 mm). However, compatibility with 23-gauge trocars is feasible by using thinner OCT probes[14] to reduce the overall thickness of the assembly. We estimate the cost of the materials (i.e., fibers and connectors) for transforming a commercial vitrector to a smart vitrector to be ~$25 US, which represents only a small fraction of its price. The components of the home-made OCT unit cost $7800 US.

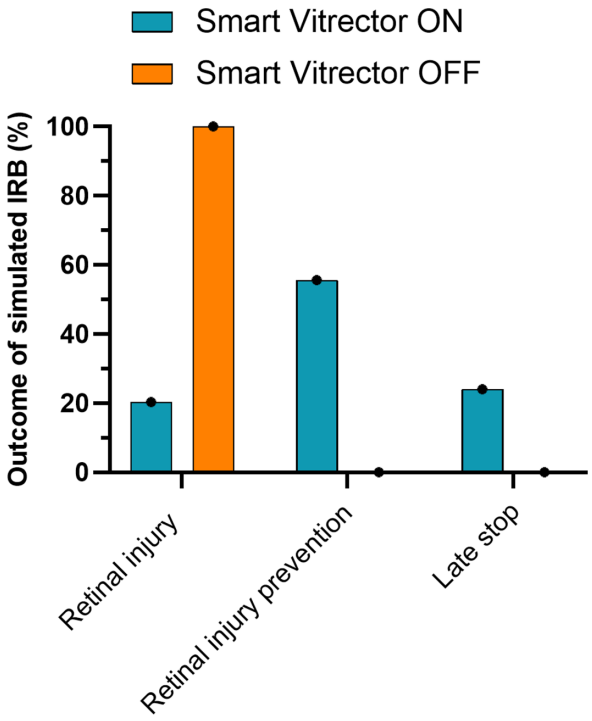

Figure 7. Outcome of simulated iatrogenic retina breaks on pigs. Fifty-four approaches were performed with the smart vitrector system "On" and three with the smart vitrector system "Off."

Considerable cost reduction, up to $3500 US, is feasible by cost-effective re-engineering of the system to downgrade components without compromising the overall performance. Altogether, these factors can favor translation of this technology to the clinic.

The smart vitrector prevented or mitigated 70.37% of simulated iatrogenic RB on pig surgeries, indicating that a subset of iatrogenic RB, linked to the late response of surgeons, can be significantly reduced. Nevertheless, efficacy improvement might be essential, because it is reasonable to expect that surgeons operating with a smart vitrector might unconsciously adopt a more aggressive operating style such as operating with higher vacuum levels or shaving the vitreous gel even closer to the vitreous base.

A subset of failures to prevent iatrogenic RB can be attributed to the 28.9 ms overall response time (i.e., from detection to pedal release) of the instrument. A-scan acquisition speed accounts for 2 ms only of the overall response time, whereas the robotic arm response accounts for the major part. This includes the servomotor response time (~20 ms), the USB and the Arduino microcontroller latency. Significant improvement of the efficacy might be attained by replacing the robotic arm by a fast (µs regime response time) electronic switch. Such an implementation would require interfering with the pedal-vitrectomy machine digital communication protocol and would reduce the response time to ~14.2 ms (i.e., software, spectrometer, and USB latency). Further improvement of the response time is feasible by using a faster OCT-tailored spectrometer.[19] Such a system can drastically reduce the component of the response time attributed to the commercial spectrometer that we used (from ~ 2 ms down to 0.2 ms). Thus further improvement of the detection algorithm should also be possible by using signal averaging. Note that vitrectomy machines present an intrinsic latency, corresponding to the actual delay between the pedal release and the actual termination of the guillotine movement and suction forces. This intrinsic latency varies among different machines and has both operating system-limited and fluid dynamics–limited components.[4,20] Using a fast imaging camera, we determined that for the settings used, the vitrectomy machine had ~200 ms latency between pedal release and guillotine stop. This latency added up to the system's response time and may account for a considerable part of the non-prevented intentional attempts at creating RB, especially those identified as "late stops," that is, retina sucked and released with no obvious injury or minor injury. The first subset of "late stops" was considered as a positive outcome by the two surgeons compared to not having a safety feature at all. Yet this is a subjective assessment implying a risk of being biased.

In this work we compare the response time of the system to the physiologically limited reaction time of the average surgeon.[5] Note that the physiologically limited reaction time represents surgeons' reaction to a visual cue (i.e., light on),[5] thus different from the time required by surgeons to react to a mobile retina. It is hard to determine the exact surgical scenarios (i.e., retina-cutter distance, suction force), for which, the physiologically limited reaction time is the primary reason for the occurrence of an iatrogenic RB. Future studies on measuring surgeons' response to a mobile retina for different surgical scenarios, could help to better identify the subset of iatrogenic RB that can be eliminated by the smart vitrector.

Based on experimentally measured flow rates for 25G vitrectors,[21] we estimate that the flow rate for our vitrectomy settings varied from 0.1 mL/min to 0.2 mL /min for 50 mm Hg vacuum and from 0.4 mL/min to 1.8 mL/min for 200 mm Hg vacuum. The range represents the two possible extremities for the status of the aspirated liquid (i.e., vitreous vs. saline solution). For our experimental settings, one can estimate that the aspirated volume by the cutter, after retinal detection, ranged from 0.04 µL to 0.87 µL. The corresponding volume can be estimated from 0.58 µL to 10.4 µL considering the reaction time of the average surgeon.

Interestingly, we observed an increased prevalence of "late stops" for approaches performed at high vacuum (200 mm Hg) compared to those performed at low vacuum (50 mm Hg) (Supplementary Table S1; surgeon 1).

The overall efficacy of the system can be further improved by improving the design of the smart vitrector's optical components. We consider that a subset of failures to prevent or mitigate simulated iatrogenic RB might have occurred because the retina entered the vitrector's orifice from a non-laser-probed area. Probed and non-probed areas of the orifice can be appreciated in Figure 1. The optical design can be improved by implementing a beam scanning approach, use of multiple probes and/or multimode fibers that can help probe the entire window from which the retina can enter. "Early stops" is another limitation that must be overcome. Although retinal damage is not exerted, "early stops" can distract surgeons and increase the duration of the surgery. Blood, bubbles, and debris scatter the probing beam, generating strong OCT signals. We thus consider them as the primary causes of "early stops." Systematic refining of the triggering condition in a controlled ex vivo setting can help identify thresholding approaches to reject such signals. For example, interrogating a sufficiently wide part of the opening that would reject point-like scattering sources and/or sharp, transient signal variations. Note that the current study was limited to a cutting speed of 6000 cuts per minute (upper limit of the machine). The prevalence of "early stops" might be higher at higher cutting speeds as an increased number of bubbles and debris might be generated. Machine learning approaches can also be implemented to improve the detection algorithm and potentially eliminate "early stops" of the cutter by differentiating blood, bubbles, and debris from retina signal. For instance, by corelating "early stop" OCT signals with corresponding "triggering" events captured by fast imaging performed in a controlled ex vivo setting.

Although further preclinical development is essential, the initial validation of the smart vitrector indicates that clinical adoption of the technology can potentially decrease the overall rate of iatrogenic RB in PPV and thus increase the therapeutic outcome of the surgery.

Acknowledgments

The authors thank the personnel of the HMR animal facility for the technical support, N. Pateromichelakis for helping us to design the pedal automation, and M. Marcoux (CRCHUM animal facility) for kindly providing us porcine eyes.

Supported by Fonds de la Recherche en Santé du Québec (253123 and 265459); Fonds de recherche en ophtalmologie de l'Université de Montréal.

Disclosure: **A. Abid,** US 63/109,040 (P); **R. Duval,** US 63/109,040 (P); **F. Rezende,** US 63/109,040 (P); **C. Boutopoulos,** US 63/109,040 (P)

References

1. Duval R, Rezaei KA. Vitrectomy surgery for primary retinal detachment. *Dev Ophthalmol*. 2014;54:174–181.
2. Wilkes SR, Beard CM, Kurland LT, Robertson DM, O'Fallon WM. The incidence of retinal detachment in Rochester, Minnesota, 1970–1978. *Am J Ophthalmol*. 1982;94:670–673.
3. Lv Z, Li Y, Wu Y, Qu Y. Surgical complications of primary rhegmatogenous retinal detachment: a meta-analysis. *PLoS One*. 2015;10(3):e0116493.
4. Charles S. Fluidics and cutter dynamics. *Dev Ophthalmol*. 2014;54:31–37.
5. Pfister M, Lue J-CL, Stefanini FR, et al. Comparison of reaction response time between hand and foot controlled devices in simulated microsurgical testing. *Biomed Res Int*. 2014;2014(March):1–8.
6. de Oliveira PRC, Berger AR, Chow DR. Vitreoretinal instruments: vitrectomy cutters, endoillumination and wide-angle viewing systems. *Int J Retin Vitr*. 2016;2:28.
7. Teixeira A, Chong LP, Matsuoka N, et al. Vitreoretinal traction created by conventional cutters during vitrectomy. *Ophthalmology*. 2010;117:1387–1392.
8. Missel PJ, Ma Y, McDonell BW, Shahmirzadi D, Abulon DJK, Sarangapani R. Simulation of vitreous traction force and flow rate of high speed dual-pneumatic 7500 cuts per minute vitrectomy probes. *Transl Vis Sci Technol*. 2020;9(8):1–15.
9. Fujimoto JG. Optical coherence tomography for ultrahigh resolution in vivo imaging. *Nat Biotechnol*. 2003;21:1361–1367.
10. Asami T, Terasaki H, Ito Y, et al. Development of a fiber-optic optical coherence tomography probe for intraocular use. *Invest Ophthalmol Vis Sci*. 2016;57(9):OCT568–OCT574.
11. Carrasco-Zevallos OM, Viehland C, Keller B, et al. Review of intraoperative optical coherence tomography: technology and applications [Invited]. *Biomed Opt Express*. 2017;8:1607.

12. Kang J, Cheon G. Demonstration of subretinal injection using common-path swept source OCT guided microinjector. *Appl Sci*. 2018;8:1287.
13. Song C, Park DY, Gehlbach PL, Park SJ, Kang JU. Fiber-optic OCT sensor guided "SMART" micro-forceps for microsurgery. *Biomed Opt Express*. 2013;4:1045.
14. Abid A, Mittal S, Boutopoulos C. Etching-enabled extreme miniaturization of graded-index fiber-based optical coherence tomography probes. *J Biomed Opt*. 2019;25(3):1.
15. Deuchler S, Wagner C, Singh P, et al. Clinical efficacy of simulated vitreoretinal surgery to prepare surgeons for the upcoming intervention in the operating room. *PLoS One*. 2016;11(3):e0150690.
16. Han S, Sarunic M V, Wu J, Humayun M, Yang C. Handheld forward-imaging needle endoscope for ophthalmic optical coherence tomography inspection. *J Biomed Opt*. 2008;13(2):020505.
17. Joos KM, Shen J-H. Miniature real-time intraoperative forward-imaging optical coherence tomography probe. *Biomed Opt Express*. 2013;4:1342–1350.
18. Mura M, Iannetta D, Nasini F, et al. Use of a new intra-ocular spectral domain optical coherence tomography in vitreoretinal surgery. *Acta Ophthalmol*. 2016;94:246–252.
19. Kim S, Crose M, Eldridge WJ, Cox B, Brown W, Wax A. Design and implementation of a low-cost, portable OCT system. *Biomed Opt Express*. 2018;:1232–1243.
20. Steel DHW, Charles S. Vitrectomy fluidics. *Ophthalmologica*. 2011;226(Suppl. 1):27–35.
21. Stanga PE, Pastor-Idoate S, Zambrano I, Carlin P, McLeod D. Performance analysis of a new hypersonic vitrector system. *PLoS One*. 2017;12(6):e0178462.